J. Fluid Mech. (1969), *vol.* 36, *part* 1, *pp.* 87–112
Printed in Great Britain

Heat transfer and transition to turbulence in the shock-induced boundary layer on a semi-infinite flat plate

By W. R. DAVIES AND L. BERNSTEIN
Department of Aeronautical Engineering,
Queen Mary College, London

(Received 30 May 1968 and in revised form 29 July 1968)

The results of experiments designed to investigate the shock-induced boundary layer on a semi-infinite flat plate are described.

Those for the laminar boundary layer are shown to be in agreement with a theory due to Lam & Crocco (1958) which describes two distinct domains, one near the shock where the flow is quasi-steady in a shock-fixed co-ordinate system and an unsteady region in which the flow characteristics approach the familiar steady state asymptotically. Experimental results are also presented for the non-laminar boundary layer. In particular the transition to turbulence in this unsteady boundary layer is discussed in some detail.

'Establishment times' for steady boundary layers are given for both laminar and turbulent flows, and their relevance to the testing times available in shock tubes is discussed. The measured heat transfer rates are compared with existing theories.

1. Introduction

The shock tube and its modifications are widely used for the generation of high enthalpy, high speed flows. One of the more prominent features of such devices, the short available test time, constitutes both an advantage and a disadvantage. It is an advantage in so far as neither the shock tube structure nor models placed in the flow suffers ablation in such a short time (of order milliseconds or less). On the other hand one is faced with serious measurement problems which have been overcome only relatively recently. Although the shock tube was invented by Vieille as long ago as 1899, it was not until the advent of electronics and high-speed data recording by means of cathode ray oscillographs that useful aerodynamic data could be obtained. Even so a fundamental problem remains.

It is well known that when a flow takes place in the vicinity of a body in an unsteady manner there is a phase lag during which the flow characteristics adjust towards the new situation. The general flow field about a body may be broadly divided into three regions: the external field, the boundary layer and the wake. The adjustment of each of these regions does not take place at a common rate because the mechanism producing change is different for each. Adjustment of the external flow field takes place largely as a result of wave propagation, which implies quasi-steadiness after a time equivalent to fluid particles travelling a few body lengths, since wave velocities are at least sonic. Adjustment of the bound-

ary-layer flow is the result of diffusion, either molecular or turbulent. This is a considerably slower process than that due to wave propagation, but the thinness of the boundary layer somewhat compensates for this. The time required for wake flow adjustment depends upon processes that are not well understood. Some features of the wake are probably established by wave propagation, its overall shape for example, others by diffusion. The critical feature is likely to be the governing mechanism for the spreading of vorticity within the wake. If wave propagation dominates, the time will be short; if the process is diffusion dominated the time may be comparatively long.

In the present paper we confine attention to the establishment of the boundary-layer flow. That the vorticity generated at the surface of a body moving relative to a fluid takes time to diffuse into the flow is well illustrated by Rayleigh's (1911) classic analysis of the laminar, viscous isochoric flow set up by the impulsive motion of an infinite flat plate in its own plane, in an initially stationary fluid. The process is an asymptotic one. That is, the final 'steady' state is reached only after an infinite time. It is possible to define a time at which the flow differs from the asymptotic state by however small a margin one desires. Indeed there is a sense in which all physical situations should be analyzed by including the time dependence, since all states have to 'come about' from a different previous state. Experience shows us, however, that in many cases the approach to the steady state is sufficiently rapid that it need not concern us, and we need only examine the steady case.

In the shock-tube environment, this is not so obvious. For example, we may be interested in simulating the steady flow past a model. We are aware that diffusion processes require time, yet the quasi-steady flow available exists for only a short time. It is essential to ascertain that the establishment of the boundary layer which forms close to the surface of the model takes place in a time which is significantly less than the available test time. Again we may expect to be faced with an asymptotic process and also with a situation in which after some finite time the departure from the final state is negligibly small.

Rayleigh's problem has already been mentioned. Other workers have developed solutions for the impulsive motion of an infinite plate in a compressible fluid (Howarth 1951 and Stewartson 1955) and for a semi-infinite† plate moved normal to its edge and in its own plane (Stewartson 1951). In these impulsive motions all particles in contact with the plate are set into motion at the same instant. In this respect they differ from the present problem. In the shock tube it is the passage of the shock which sets the fluid in motion and different positions on the model are affected at different times. This is partly true of the semi-infinite flat plate case analyzed by Stewartson (1951) but for different reasons. In that case different parts of the plate 'become aware' of the leading edge at different times.

In the shock tube, clearly the simplest model is a stationary flat plate of infinite extent aligned parallel or perpendicular to the plane shock travelling down the shock tube. In the first case the solution is trivial in the present context. The shock is reflected to leave stagnant gas in contact with the plate. In the second the situa-

† The term 'semi-infinite' is used to imply that the plate occupies say only the positive half of the plane yOz: that is Ox_+ is a cross-section.

tion is essentially that which exists on the wall of a rectangular cross-section shock tube in which corner effects are ignored.† The boundary layer which grows from the foot of the shock is clearly quasi-steady in a co-ordinate system which moves with the shock. This problem has been analyzed by several workers (see, for example, Mirels 1956 and Ackroyd 1967). It is discussed more fully in §2 since it has a direct bearing on the present problem. Many experiments have been carried out which give confidence in Mirels's solutions.

The next stage in complexity is a semi-infinite flat plate aligned with its plane normal and its edge parallel to the shock. It is this case which forms the subject of the present investigation. In the neighbourhood of the model the flow begins when the shock arrives at the leading edge of the plate. A boundary layer then forms on the surface of the plate and this boundary layer has two 'leading edges', one at the foot of the shock, the other at the leading edge of the plate. We might intuitively expect all those particles initially downstream of the plate leading edge to behave in exactly the same way as particles on the shock-tube wall. This has been formally shown to be so in an elegant analysis by Lam & Crocco (1958) which is discussed in §2. After an infinite time we expect a steady state to be reached, and Lam & Crocco have succeeded in describing the approach to this asymptote for the laminar boundary layer. We shall describe an experimental investigation designed to test the results of Lam & Crocco and confirm that 'steady' boundary layers can indeed be set up around a simple model mounted in a shock tube in spite of the short duration of quasi-steady flow. We imply here that after a finite time significantly shorter than the available test time, the boundary-layer characteristics differ little from their asymptotic values.

In order to demonstrate this the theoretical predictions of Mirels and of Lam & Crocco are discussed in some detail in the following section. An earlier, less general solution of the present problem due to Dem'yanov (1957) is also briefly mentioned. Attention is focused on those analytical results which have a direct bearing on the measurements actually made in the experimental investigation. In particular the predictions regarding heat transfer rate and surface temperature history are discussed for subsequent comparison with the experiments.

The analytical solutions mentioned so far have all been for the case of the laminar boundary layer. In practice of course the boundary layer may not remain laminar. Mirels (1956) has produced a semi-empirical solution for the turbulent boundary-layer growth behind the shock on a shock-tube wall. Lack of relevant experimental data necessitated his use of steady incompressible flow data. Spence & Woods (1960) used steady compressible flow data in an attempt to solve the same problem, but all such approaches are open to criticism (see Bernstein 1963*a*). In the present problem not only did no experimental data exist, but also where Mirels' problem is steady in a shock fixed co-ordinate system, this one is essentially time dependent in the region of the plate leading edge. Thus no semi-empirical formulation could be made.

Some measurements have been made and are reported here which show that the 'flow establishment time' is shorter for the turbulent than for the laminar

† Strictly, such a shock tube would have to be infinitely long, so that the presence of the driver gas did not complicate the situation.

boundary layer. This is to be expected in view of the better mixing in a turbulent boundary layer; that is, turbulent diffusion is more efficient than molecular diffusion at spreading vorticity. Some interesting results are also reported concerning the nature of the transition process in this boundary layer with two leading edges. These results are shown to be consistent with the relevant features of the boundary layer as predicted by Lam & Crocco.

2. Theory

Let us suppose that a semi-infinite flat plate is immersed in a stationary compressible gas of infinite extent whose thermodynamic state is characterized by suffix $_1$, and let the origin of a co-ordinate system (x, y) lie in the leading edge of the plate with the plate cross-section occupying the positive x-axis. A plane shock wave normal to the x-axis approaches with velocity w_1 in the positive x-direction and arrives at the plate leading edge at time $t = 0$. For $t > 0$ the shock travels over the plate. The gas velocity behind the advancing shock is denoted† by u_2. The shock strength is characterized by the shock Mach number $W_{11} = w_1/a_1$, where a_1 is the sound speed ahead of the shock, or by the velocity ratio w_1/u_2 which proves to be more useful in the present problem.

(i) *Laminar boundary layer*

Making the assumptions that both the Prandtl number $\sigma = \mu c_p/k$ and $\rho\mu$ are constant throughout the boundary layer which develops between the foot of the shock and the leading edge of the plate (figure 1), Lam & Crocco (1958) have succeeded in analyzing the case when the boundary layer is laminar. Here μ is the viscosity, ρ the density, k the thermal conductivity and c_p the isobaric specific heat capacity of the gas. The boundary-layer equations are first transformed so that the independent variables are (α, β, γ) given by

$$\alpha = \frac{x}{u_2 t}; \quad \beta = \frac{u}{u_2}; \quad \gamma = \frac{u_2^2 t}{\nu_2}, \tag{1}$$

where ν denotes the kinematic viscosity of the gas and suffix $_2$ denotes values outside the boundary layer and behind the shock. Shear stress and enthalpy are used as dependent variables.

The region of interest in the (α, β, γ) space is then a right rectangular prism open in the $+\gamma$ direction, more particularly, the solution of the boundary-layer equations is required in the region

$$0 \leqslant \alpha \leqslant w_1/u_2; \quad 0 \leqslant \beta \leqslant 1; \quad \gamma \geqslant 0. \tag{2}$$

They show that this region may be divided into two parts separated by the singular plane $\alpha = 1$. This singular plane clearly maps onto the (x, t) plane as the path of a particle originating at the plate leading edge $x = 0$, and travelling outside the boundary layer with velocity u_2. All particles for which $1 \leqslant \alpha \leqslant w_1/u_2$ originate at $x \geqslant 0$, that is 'on the plate', and have no knowledge of the plate lead-

† Where possible the notation conforms with standard shock tube practice.

ing edge. The boundary layer induced by the shock in this region is precisely that formed on a plate without a leading edge and this is known to be quasi-steady in a co-ordinate system moving with the shock (Mirels 1955, 1956).

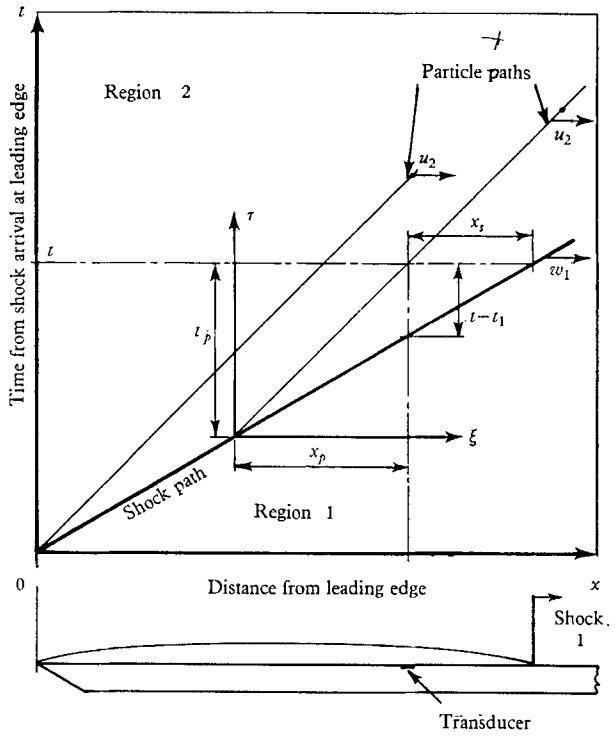

FIGURE 1. The flow in the distance–time plane illustrating the co-ordinate system.

We thus have two regions defined: a quasi-steady region

$$1 \leqslant \alpha \leqslant w_1/u_2; \quad 0 \leqslant \beta \leqslant 1; \quad \gamma \geqslant 0 \tag{3a}$$

and an interaction region

$$0 \leqslant \alpha \leqslant 1; \quad 0 \leqslant \beta \leqslant 1; \quad \gamma \geqslant 0. \tag{3b}$$

The quasi-steady region. The quasi-steady region is only briefly discussed by Lam & Crocco but has been analyzed by Mirels (1955, 1956) in considerable detail. Their results are in excellent agreement.

Mirels gives an expression for the heat transfer rate into the plate as

$$\dot{q}_w = s'(0)\,[T_w - T_r]\frac{c_p}{\sigma}\sqrt{\left(\frac{\rho_w \mu_w (w_1 - u_2)}{2x_s}\right)}, \tag{4}$$

where x_s is the distance from the shock, T_w is the temperature of the surface of the plate, T_r is the recovery temperature defined by

$$T_r = T_2\{1 + r(0)\,\tfrac{1}{2}(\overline{\gamma} - 1)\,M_2^2\}, \tag{5}$$

$\overline{\gamma}$ is the ratio of principal specific heat capacities, M_2 is the flow Mach number behind the shock, $r(0)$ and $s'(0)$ are functions of the boundary-layer velocity profiles evaluated by Mirels and suffix $_w$ denotes values at the surface of the plate.

From the geometry of the (x, t) diagram (figure 1) we see that x_s is related to the distance x_p travelled by a particle in the inviscid flow since it was first set into motion by the shock, by

$$x_s/x_p = (w_1 - u_2)/u_2. \tag{6}$$

If we define a Stanton number St, by

$$St = \frac{\dot{q}_w}{\rho_2 u_2 c_p (T_r - T_w)} \tag{7}$$

and a Reynolds number Re_{x_p} by

$$Re_{x_p} = \frac{u_2 x_p}{\nu_2}, \tag{8}$$

we may write (4) in the form

$$St\sqrt{Re_{x_p}} = -\frac{s'(0)}{\sigma\sqrt{2}}\sqrt{\left(\frac{\rho_w \mu_w}{\rho_2 \mu_2}\right)} \tag{9}$$

for

$$1 \leqslant \alpha \leqslant w_1/u_2.$$

Although in his early work Mirels assumed $\rho\mu$ to be constant in order to integrate the equations, there is no need to carry this assumption into (9). In later work, Mirels (1961) was able to relax this assumption. He also produced interpolation formulae for $r(0)$ and $s'(0)$ which closely fit his numerical results. Equation (9) is thereby modified to become

$$St\sqrt{Re_{x_p}} = \frac{s'(0)}{\sigma\sqrt{2}}\left\{\frac{\rho_w \mu_w}{\rho_2 \mu_2}\right\}^{0\cdot235}, \tag{9a}$$

with

$$s'(0) = 0\cdot489\sqrt{(1 + 1\cdot664\Gamma_{21})}\,\sigma^{0\cdot48+0\cdot022\Gamma_{21}} \tag{10}$$

and

$$r(0) = \sigma^{0\cdot39-0\cdot023\Gamma_{21}}, \tag{11}$$

where $\Gamma_{21} = w_1/(w_1 - u_2)$, is the density ratio across the shock.

For a given strength shock, the right-hand side of (9*a*) is independent of time. We thus expect that, for a given shock,

$$\dot{q}_w\sqrt{x_p} = \text{constant, in the range } 1 \leqslant \alpha \leqslant w_1/u_2.$$

Now suppose the shock arrives at a particular station x on the plate at a time t_1, after passing the leading edge. Then

$$\frac{x_p}{t - t_1} = \frac{u_2 w_1}{w_1 - u_2}. \tag{12}$$

Thus

$$\dot{q}_w\sqrt{(t - t_1)} = \text{constant} \tag{13}$$

in the range $1 \leqslant \alpha \leqslant w_1/u_2$ for a particular shock. The time $(t - t_1)$ is that displayed on an oscillograph for examining the output of a transducer placed at this point on the plate. A heat transfer rate gauge would therefore be expected to indicate a very high rate† of heat transfer as the shock arrived, and this should then diminish as $(t - t_1)^{-\frac{1}{2}}$.

† The infinite rate predicted by equation (13) as $t \to t_1$ cannot occur in practice because the shock thickness is finite. At the foot of the shock the assumptions upon which the boundary-layer equations are based are violated.

The variation of surface temperature with time depends upon the thickness of the plate. If the latter is much thicker than the thermal boundary layer in the wall (a condition easily achieved in practice) then it is well known that with a heating rate as given by (13) the wall temperature T_w is constant (see, for example, Carslaw & Jaeger 1947).

The interaction region. The interaction region ($0 \leqslant \alpha \leqslant 1$) is extensively studied by Lam & Crocco. The assumption $\rho\mu$ = constant uncouples the equations of momentum and energy conservation so that these may be solved separately. It is formally demonstrated that the flow in the quasi-steady region is unaffected by the interaction region and that the proper solution in the interaction region requires the prior solution of the quasi-steady region since conditions on the singular plane $\alpha = 1$ are needed as boundary conditions in addition to those at the plate leading edge.

Solutions of the boundary-layer equations were obtained by Lam (1959) for several values of w_1/u_2 using a numerical integration procedure. Results are presented for the skin friction coefficient $C_f(\alpha)$ in the form $C_f(\alpha)\sqrt{Re_x}$, the Reynolds analogy factor $Ra(\alpha, \sigma)$, the boundary-layer momentum thickness $\theta(\alpha)$ and the boundary-layer form factor $\mathscr{H}(\alpha) = \delta_1/\theta$, where $\delta_1(\alpha)$ is the displacement thickness. The Reynolds analogy factor is defined by

$$Ra = 2St/C_f. \tag{14}$$

From the tabulated data one may construct curves of $St\sqrt{Re_x}$ as a function of α for several values of the Prandtl number σ.

At $\alpha = 1$ the distance x_p moved by a particle is equal to its distance x from the leading edge of the plate. We should thus expect to find

$$\{St\sqrt{Re_x}\}_{\alpha=1} = \{St\sqrt{Re_{x_p}}\}_{\text{Mirels, } \rho\mu = \text{const.}}$$

and the two sets of results agree very closely.

As $t \to \infty$ and the shock is far from the leading edge of the plate, we should expect the particles in the neighbourhood of the leading edge to have 'forgotten' how they were set in motion. In other words, we expect the flow near the leading edge of the plate to resemble the steady, laminar, compressible flow over a flat plate analyzed by Crocco (see Young 1953, chapter X). This is indeed the case, the Crocco steady flow solution is the asymptotic solution as $\alpha \to 0$† of the unsteady flow equations examined by Lam & Crocco.

In fact $St\sqrt{Re_x}$ remains sensibly constant in a range $0 \leqslant \alpha \leqslant \alpha_1$; the value of α_1 is arbitrary until one specifies the degree of approach of $[St\sqrt{Re_x}]_{\alpha_1}$ to its asymptotic value. For $\sigma = 0{\cdot}7$, $St\sqrt{Re_x}$ remains constant to within 5 % over the range $0 \leqslant \alpha \leqslant 0{\cdot}3$ for a wide range of shock strengths.

Young (1953) discusses in some detail the effects of freestream Mach number and wall temperature when $\rho\mu \neq$ constant. He gives an approximate formula for $C_f\sqrt{Re_x}$ which may be used with a modified Reynolds analogy to give for the steady heat transfer rate

$$St\sqrt{Re_x} = 0{\cdot}332\sigma^{-\frac{2}{3}}\{0{\cdot}45 + 0{\cdot}55T_w/T_2 + 0{\cdot}09(\bar{\gamma} - 1)\,\sigma^{\frac{1}{2}}M_2^2\}^{\frac{1}{2}(\omega-1)}, \tag{15}$$

where ω is the index in the power-law viscosity–temperature relation.

† Note that $\alpha \to 0$ must be taken to imply $t \to \infty$ rather than $x \to 0$, since the boundary-layer formulation breaks down close to the plate leading edge.

Over the range $0 \leqslant \alpha \leqslant 0{\cdot}3$ in which $St\sqrt{Re_x}$ is sensibly constant, we infer that for a particular point on the plate (x fixed), the heat transfer rate $\dot{q}_w$ is constant for a given shock. The solution to the conduction equation for a constant heating rate of a semi-infinite solid, to which the experimental situation closely approximates, is well known (Carslaw & Jaeger 1947); the surface temperature T_w increases in proportion to the square root of time

In the times of practical interest in a shock tube, the change in T_w is very much smaller than T_w. Thus, in evaluating the right-hand side of (15), T_w is taken to be equal to T_1, the temperature of the quiescent gas before the arrival of the shock.

Lam experienced some technical difficulty in the numerical integration of the equations. An analysis based on the momentum integral equation was therefore developed to provide a 'correction procedure'. The singularity $\alpha = 1$ of the detailed analysis becomes a singular point $\alpha = \alpha^*$ in the momentum integral approach and this enabled both boundary conditions (at $\alpha = 0$ and $\alpha = w_1/u_2$) to be satisfied simultaneously, though there is a discontinuity in slope at $\alpha = \alpha^*$. The singularity is shown to be the root of the equation

$$\alpha^* = \theta(\alpha^*)/\delta_1(\alpha^*) = 1/\mathscr{H}(\alpha^*). \tag{16}$$

On the further assumption that the dimensionless momentum and displacement thicknesses are constants, that is, assuming 'similar solutions', they show that in the range $0 \leqslant \alpha \leqslant \alpha^*$,

$$C_f\sqrt{Re_x} = \sqrt{(2\theta)},$$

the well-known Crocco value. This implies that the boundary layer growing from the leading edge of the plate is 'steady' as far as $\alpha = \alpha^* = 1/\mathscr{H}(\alpha^*)$. Lam's numerical solutions for the case $\rho\mu =$ constant show that $\alpha^* \approx 0{\cdot}40$ for all shock strengths. Compared with the previously quoted value $\alpha_1 = 0{\cdot}3$ as an approximate 'upper' bound for constant $St\sqrt{Re_x}$, the momentum integral approach gives somewhat optimistic results.

Dem'yanov (1957) has also considered the present problem. His approach was somewhat different but he too employed a numerical integration procedure. He also considered the solution of the momentum integral equation and his results are essentially in agreement with those of Lam & Crocco.

We may conveniently summarize these results by restricting our attention to what happens at a particular station on the plate as the shock arrives and then passes 'downstream'. This will help in the interpretation of the output, as a function of time, of a heat transfer rate gauge placed at this station, which is what is displayed on an oscillograph.

As the shock arrives (a time x/w_1 after passing the leading edge of the plate) there is a step-rise in temperature of the gas adjacent to the surface and therefore there is a jump in surface temperature. In theory the corresponding heating rate is infinite but in practice there is some rounding-off due to the finite shock thickness; the heat transfer rate to the wall, however, is very large. After the shock passage, the heat transfer rate varies inversely as the square root of the time since shock passage, until the arrival of particles which originated at $x = 0$ (i.e. until the arrival of the $\alpha = 1$ characteristic). The corresponding surface temperature

remains constant at its value just after shock passage. Thereafter the heat transfer rate will vary with time indefinitely influenced by both the shock and the leading edge of the plate and the surface temperature will rise. However, after a time corresponding to $\alpha \approx 0{\cdot}3$, the heat transfer rate will remain sensibly constant while the surface temperature rises in proportion to the square root of time (provided of course that it does not rise too far).

Idealized surface temperature and heat transfer rate variations are shown in figure 2 (*a*).

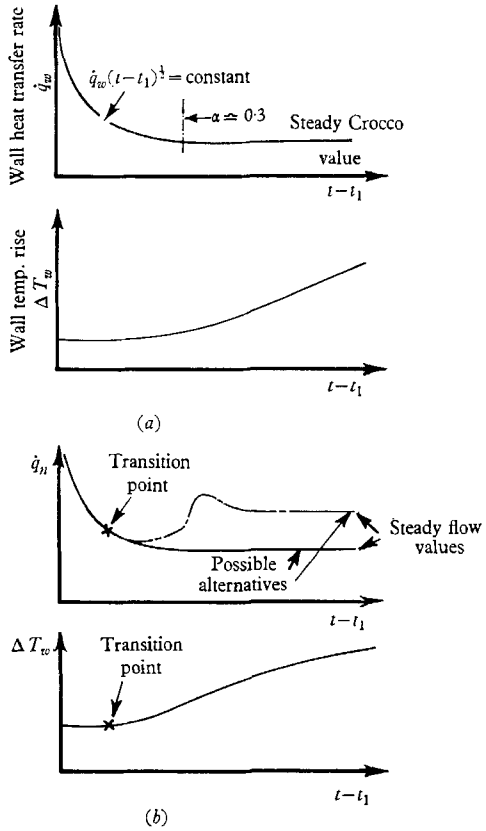

FIGURE 2. Anticipated oscillosope records for (*a*) the laminar and (*b*) the non-laminar boundary layer.

(ii) *Transitional boundary layer*

The analyses so far discussed have been carried out on the assumption that the boundary layer is laminar. It may not remain so in practice. No analytical procedure is available for predicting the behaviour of a time-dependent non-laminar boundary layer. However, one may discuss it from a phenomenological standpoint. The laminar boundary layer becomes unstable to small disturbances when the Reynolds number based upon some measure of its thickness exceeds a certain critical value. In the steady boundary layer growing on a flat plate, distance from the leading edge is a convenient measure of the boundary-layer thickness. In an unsteady boundary layer this is not sufficient, so that transition is best discussed

directly in terms of the thickness itself. Fortunately this is very convenient in the present problem because the boundary layer has a position of maximum thickness. Whatever the value of the critical Reynolds number Re_c, for given external flow conditions, transition will first occur where the boundary layer at its maximum thickness equals the critical value. According to the results of Lam the maximum momentum thickness $\tilde{\theta}$ of the laminar boundary layer occurs in the range $0{\cdot}57 \leqslant \alpha \leqslant 0{\cdot}60$ for a very wide range of shock strengths. Thus we should expect non-laminar flow to appear first at this value of α (though there may

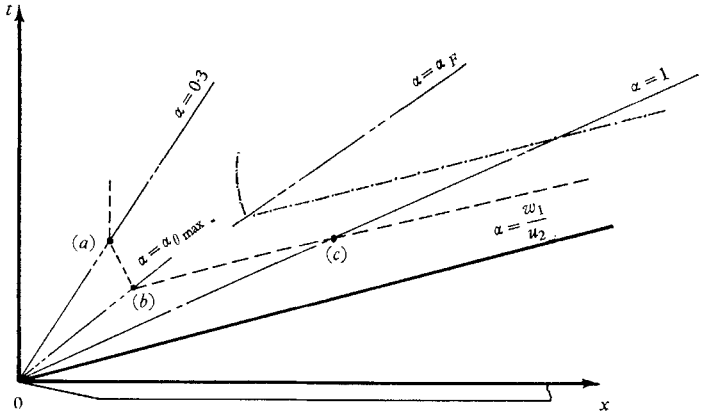

FIGURE 3. Onset of non-laminar flow. – – – –, $\theta = \theta_{\text{crit}}$ = transition path; —·—·—, 'path' of fully developed turbulence.

not be a transducer at just the position where both $\alpha = \alpha(\tilde{\theta}_{\max})$ and $\tilde{\theta}_{\max} = \tilde{\theta}_{\text{crit}}$ simultaneously). The boundary layer at any point on the plate thickens further with time, so that we should expect non-laminar flow to spread in both directions in such a way that only where $\tilde{\theta} < \tilde{\theta}_{\text{crit}}$ is the boundary-layer laminar. The spread towards the shock takes place in a non-uniform manner until the 'transition point' reaches the $\alpha = 1$ characteristic. This 'forward movement' may be specified by examination of the boundary-layer thickness profiles as a function of time as given by Lam. Once transition arrives at the $\alpha = 1$ characteristic, it remains a constant distance behind the shock, since in the region

$$1 \leqslant \alpha \leqslant w_1/u_2,$$

the laminar boundary-layer thickness depends only upon x_s, the distance from the shock.

In an analogous fashion, the transition point will also move towards the leading edge of the plate but, since the laminar boundary layer has to all intents and purposes reached its asymptotic state at $\alpha \approx 0{\cdot}3$, transition will not move nearer the leading edge than the value of x corresponding to $\alpha \approx 0{\cdot}3$. This behaviour is illustrated schematically in figure 3 on an (x, t) diagram, where the line $\tilde{\theta}$ = constant has been sketched between $\alpha = 0{\cdot}6$ and $\alpha = 0{\cdot}3$.† In a practical situation, the line $\tilde{\theta}$ = constant probably has curvature of opposite sense to that shown,

† The foregoing argument is of course based upon the assumption that the velocity profile has a secondary effect on transition in this flow. This should not lead to serious error.

so that it becomes asymptotic to a line $x =$ constant. This could arise if the thickening of the boundary layer at transition fed disturbances upstream which modified the laminar boundary layer immediately ahead.

The output response of a heat transfer rate gauge will depend upon where it is situated in relation to the points (*a*), (*b*) and (*c*) on figure 3. A thermometer will indicate a surface temperature rise at transition at all positions but for positions between (*a*) and (*c*) the temperature will already be rising, so it is unlikely to be a very noticeable effect.

For $x > x_c$, the heating rate is falling as $(\text{time})^{-\frac{1}{2}}$ in the laminar region. As the boundary layer undergoes transition, the heating rate may continue to fall, but at a slower rate. The subsequent behaviour depends upon when the turbulence becomes fully developed.

For $x_a \leqslant x \leqslant x_c$ the change in the heating rate at the surface will depend upon the relative effectiveness of two opposing tendencies; the local thickening of the boundary layer will tend to reduce $\dot{q}_w$ while the enhanced mixing will tend to increase it. Since the boundary layer thickens little with time between (*a*) and (*b*), it is likely that $\dot{q}_w$ will actually increase slightly. Between (*b*) and (*c*) it may continue to fall, particularly near (*c*), and there may be a region on the plate in which $\dot{q}_w$ remains more or less steady before rising as the turbulence level increases. This steadiness would be fortuitous because the boundary layer in this region is strongly time dependent.

(iii) *Turbulent boundary layer*

For all positions $x > x_a$, the flow is expected to become non-laminar after a time indicated by the 'transition line' in figure 3.

In the neighbourhood of the leading-edge of the plate, at positions x only slightly greater than x_a, the state of the *steady* boundary layer is transitional in character. But at other downstream positions the boundary layer flow will ultimately become fully turbulent. The smallest value of x at which fully turbulent flow eventually occurs should correspond with the value obtained in the steady flow over a flat plate with a leading edge. The boundary-layer momentum thickness $\bar{\theta}$ at this position may be inferred, in principle, from steady data but because the growth of the unsteady boundary layer in the transition region is unknown, it is not possible to construct a curve (similar to the 'transition line' of figure 3) which indicates the onset of fully turbulent flow in the boundary layer.

However we should expect such a curve to exist, and there appears to be no *a priori* reason why it should not be similar in shape to that describing the first appearance of non-laminar flow at any point on the plate. Such a hypothetical line is shown schematically in figure 3.

Once the boundary layer has become fully turbulent we may expect the heat transfer rate near the leading edge (but downstream of transition) to assume its steady 'asymptotic' value fairly rapidly. This is inferred on the grounds that the process in laminar flow is sensibly complete by the arrival of the $\alpha = 0{\cdot}3$ characteristic and, since turbulent diffusion is a more efficient mixing process than molecular diffusion, we might expect the steady state to correspond to a somewhat higher value, $\alpha = \alpha_F$, say.

These steady rates of heat transfer should correlate with other workers' data where this is available. Several workers have produced correlation formulae for the skin-friction coefficient, based on empirical data. Spence (1960) in particular has also produced a Reynolds analogy factor for turbulent heat transfer. Using his formulae, we may write

$$St_m(Re_{mx})^{\frac{1}{5}} = 0{\cdot}0296Ra, \tag{17}$$

where the Stanton and Reynolds numbers are based upon properties at the mean specific enthalpy h_m, defined by

$$h_m = h_2(0{\cdot}55 + 0{\cdot}45(h_w/h_2) + 0{\cdot}035M_2^2) \tag{18}$$

and $Ra = 1{\cdot}18$ for the present data.

In the present case $h_w = h_1$, the value ahead of the shock, and since little error is introduced by assuming the gas to be perfect, we may take h proportional to T.

In the region near the shock, and for $\alpha \geqslant 1$, the boundary layer should behave in an identical manner to that on a shock tube wall. We might therefore expect that the 'fully turbulent' line will follow a path in the (x, t) diagram parallel to both the 'transition line' and the shock trajectory. The fully turbulent boundary layer growing from the foot of the shock on the shock tube wall has been analyzed by Mirels (1956), who used steady incompressible data for the shear stress function. Using Reynolds analogy, he predicted that

$$St\, Re_x^{\frac{1}{5}} = \text{constant}, \tag{19}$$

the constant depending upon the shock strength. The one-fifth power corresponds to a one-seventh power law velocity profile in a co-ordinate system moving with the shock. Hartunian, Russo & Marrone (1960) have carried out measurements of heat transfer rate to the walls of a shock tube which largely confirm this relation, so we may expect similar results for $\alpha \geqslant 1$.

In the range $\alpha_F < \alpha < 1$, the behaviour is unknown, and whether $\dot{q}_w$ falls or rises toward its final steady value depends upon the particular position on the plate. The latter governs the relative magnitudes of the heat transfer rate as the $\alpha = 1$ characteristic arrives and the asymptotic steady value appropriate to the distance x from the leading edge of the plate.

Semi-empirical relations of the type quoted in (17) and (19) are based upon the assumption that the boundary layer is turbulent from the leading edge. Accordingly, when making comparisons with experimental data obtained under conditions where part of the boundary layer is laminar, a correction is usually necessary. This correction takes the form of evaluating a 'false origin' for the turbulent boundary layer. The procedure is well documented and the correction is often small.

3. Experimental investigation

(i) *Apparatus*

An experimental investigation of the problem has been carried out on a flat plate mounted in the low pressure section of the shock tube which forms part of the Queen Mary College hypersonic shock tunnel. The shock tube driver chamber

is 2·44 m long and 108 mm diameter. The low pressure section, or channel, has a uniform cross section, 76·2 mm square, and is approximately 9·5 m long. Cold hydrogen was used to drive shocks in nitrogen.

The flat plate model which was made of steel, has a sharp leading edge formed by a 30° included angle. It was mounted so as to span the channel and its leading edge was 9·17 m from the main diaphragm. Inset into its upper surface is a Pyrex plate on which have been deposited thin-film platinum resistance thermometers manufactured using Hanovia Liquid Bright Platinum 05. The twelve resistance thermometers are situated at distances from the leading edge between 17·5 mm and 115·1 mm and they occupy approximately 30 % of the span, being symmetrically placed about the central chord line. The resistance of each film is of order 100 Ω. They are supplied with a constant current of about 10 mA.

The output voltage representing a temperature change was displayed directly on one beam of a Tektronix 551 cathode ray oscilloscope. The same voltage was also led to the input terminals of a heat transfer rate analogue circuit similar to that of Meyer (1960); the output signal was displayed on the second beam of the cathode ray oscilloscope.

The thin film gauges and corresponding analogue circuits were calibrated together by investigating their response to a range of known heating rates obtained by discharging a condenser through a Wheatstone bridge circuit, one arm of which was formed by the resistance thermometer. The active area of each gauge was determined from an enlarged photograph of the model.

The equilibrium thermodynamic state of the gas behind the shock is completely determined by the initial channel gas pressure and the temperature and the shock speed. The pressure p_1 was measured using a Wallace & Tiernan bourdon gauge and the temperature T_1 was assumed equal to room temperature. The shock speed was measured by timing the shock passage over a distance spanning the model of 254 mm using a pair of piezo-electric shock detectors and trigger amplifiers together with a chronometer having a resolution of 0·1 μs (Bernstein & Goodchild 1967).

Further details of the apparatus and its calibration are given by Davies (1968).

(ii) *Experimental results*

The rather large leading edge wedge angle used on the model gives rise to flow conditions which do not strictly satisfy the assumptions made in the analysis. When the shock-induced flow is subsonic the upper, flat surface flow is affected by the lower surface. This is also true of those cases investigated for which $M_2 > 1$. The highest flow Mach number M_2 investigated was about 1·84. The largest wedge angle for which the bow shock wave is attached at this Mach number is about 20°. Thus the bow shock would be detached for all the conditions investigated (for which $M_2 > 1$) and the upper surface flow was not strictly independent of that on the lower wedge surface. Moreover, the local flow conditions on the flat surface would be modified since the gas initially upstream of the leading edge ($\alpha < 1$) would pass through this bow shock. Even were the lower wedge surface shock attached, the formation of the boundary layer itself introduces a displacement

effect which gives rise to a shock, albeit attached. No account of this shock is taken in the theory. It is, however, likely to be weak, since except at very low densities the rate of boundary-layer growth with distance from the leading edge is small. Under such conditions the angle the shock makes with the oncoming flow is close to the Mach angle. Thus some measure of the 'bluntness effect' may be obtained by examining schlieren photographs of the flow and noting the extent of that portion of the shock which is highly curved. The curved region gives rise to an entropy layer which may significantly alter the downstream flow.

The extent of this deficiency in the experimental arrangement is not easy to determine. That the effect was small for all the conditions investigated is inferred from the good agreement between theory and experiment for the laminar boundary-layer case.

Further evidence in support of this conclusion is afforded by the schlieren photograph reproduced in figure 14, plate 1. This was taken at a shock Mach number of 5·3 using a different model with a wedge angle of 22·5°, in a smaller shock tube, since the 76·2 mm square shock tube is not equipped with windows.

In addition the mounting is somewhat different, the instrumented plate being supported by dowels located in the side walls of the shock tube. (The support for the model shown in figure 14 is hollow so that the undersurface flow is not completely blocked.)

The Mach number M_2 of the flow behind the incident shock is 1·86, so that the undersurface shock is close to attachment. The upper surface shock is *highly* curved over a very small region only and the angle the linear portion makes with the oncoming flow is only about 5° greater than the Mach angle. The reflexion of this wave from the upper wall of the shock tube is very close to the Mach angle and it decays rapidly. We may infer that the entropy gradients in the flow are not large except in the region very close to the leading edge. The effect of the bow shock on the heat transfer rate is thus likely to be small at distances greater than about two plate thicknesses from the leading edge which corresponds approximately to the position of the leading usable gauge on the instrumented model.

The experiments were performed over a range of shock Mach numbers W_{11} with a variety of initial channel pressures p_1. The tests fall into three groups according to which parameters were varied. In the first group W_{11} was varied by adjusting the channel pressure p_1 at constant driver pressure, and conditions were examined at two fixed positions on the plate. In the second group conditions were examined at several stations on the plate at fixed values of shock Mach number and channel pressure. One gauge was used throughout this series as a monitor. In the final group p_1 (and hence Reynolds number) was varied while conditions were investigated at two particular stations at fixed shock Mach numbers.

In general terms the 'output waveforms' of the transducers accord qualitatively with those predicted in § 2. The jump in temperature followed by a plateau and then a slow rise is paralleled by an initially high heat transfer rate at shock passage followed by a fall, the rate of which diminishes with time as long as the boundary layer remains laminar, but may increase again if non-laminar flow appears.

The initial step rise in temperature and the corresponding heat transfer rate which is inversely proportional to the square root of time since shock passage broadly confirm Mirels's results. Numerical comparisons are shown in figure 5 where $St\sqrt{Re_{x_s}}$ is plotted against W_{11} and in figure 4 where $\Delta T_w/\sqrt{p_1}$ is plotted

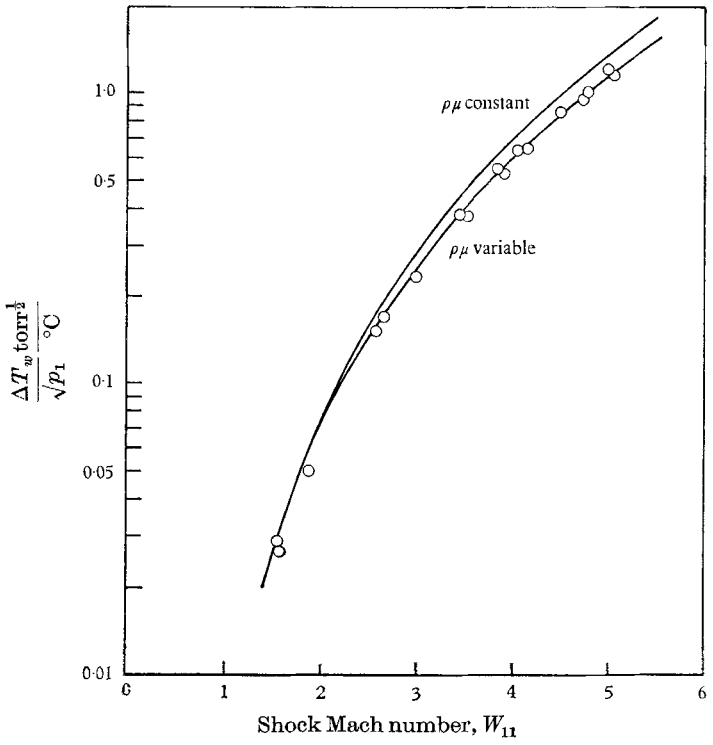

FIGURE 4. Initial wall temperature rise. ——, Mirels (1956, 1961).

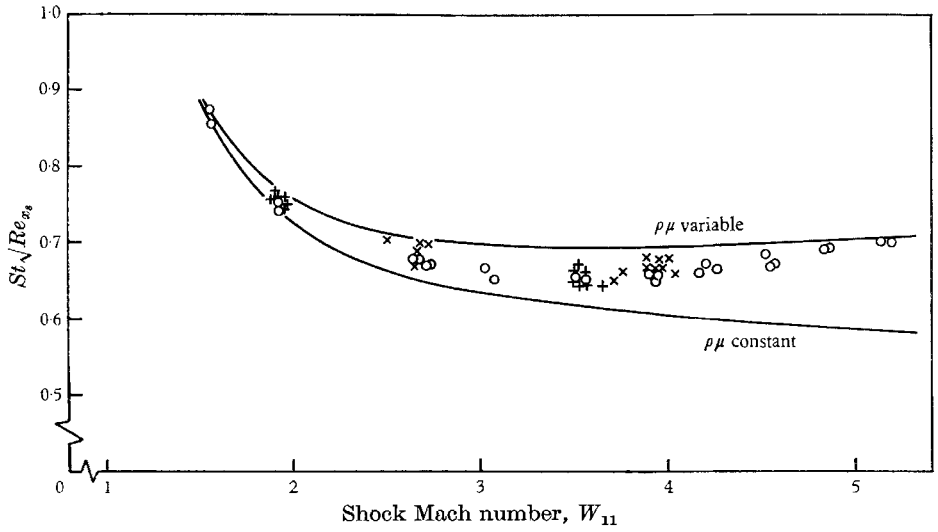

FIGURE 5. Comparison of results with Mirels's analysis for the quasi-steady laminar boundary layer. Experimental results: ○, group 1; +, group 2; ×, group 3.

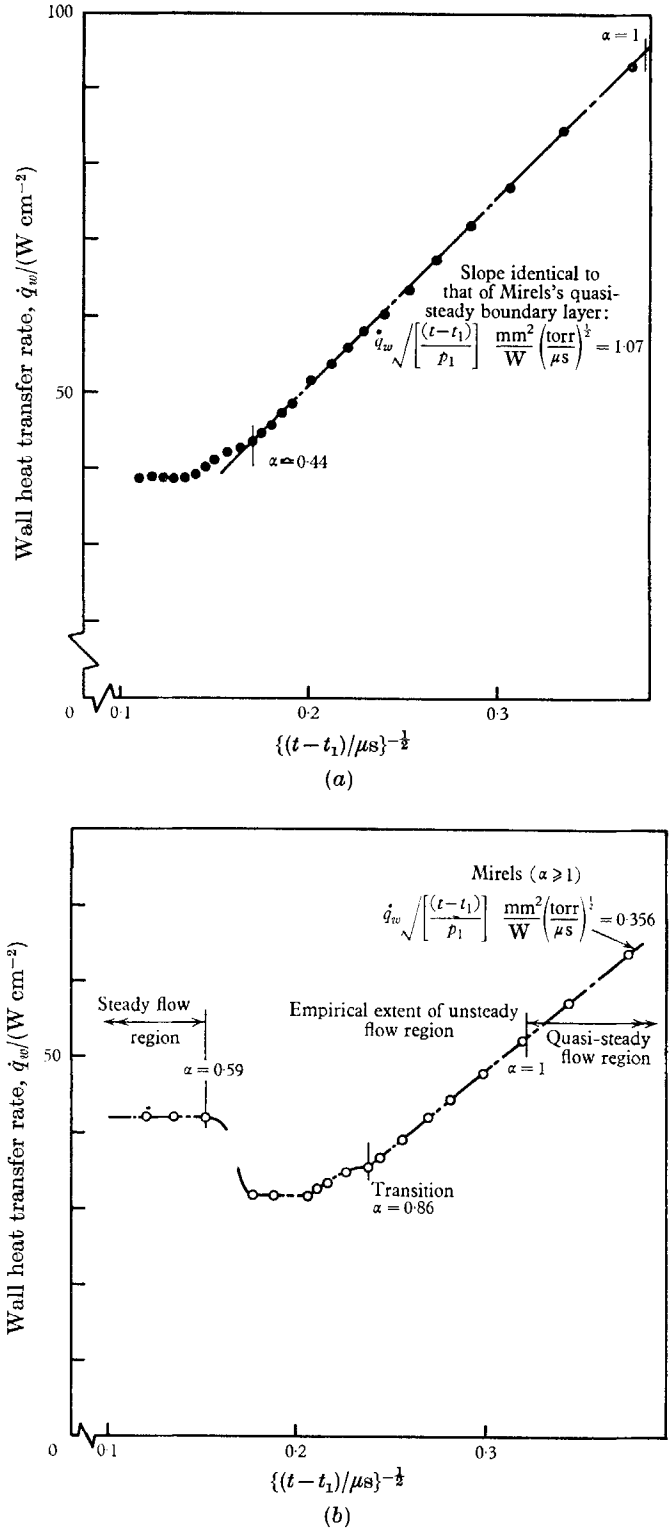

FIGURE 6. Wall heat transfer rate in the interaction region. (*a*) Boundary layer becomes steady laminar. $W_{11} = 5{\cdot}18$, $p_1 = 5{\cdot}5$ torr, $x = 34{\cdot}9$ mm. (*b*) Boundary layer becomes steady non-laminar. $W_{11} = 3{\cdot}56$, $p_1 = 34$ torr, $x = 44$ mm.

against W_{11}. All the data reduction has been carried out using the imperfect gas properties behind the shock (Bernstein 1963*b*) together with the thermodynamic properties of nitrogen as given by Woolley (1956). Better agreement in figure 4 suggests either some errors in the calibration of the analogue network, or it may reflect the fact that Mirels's interpolation formulae for $\rho\mu$ variable were based upon computations for air, whereas these data were obtained in nitrogen.

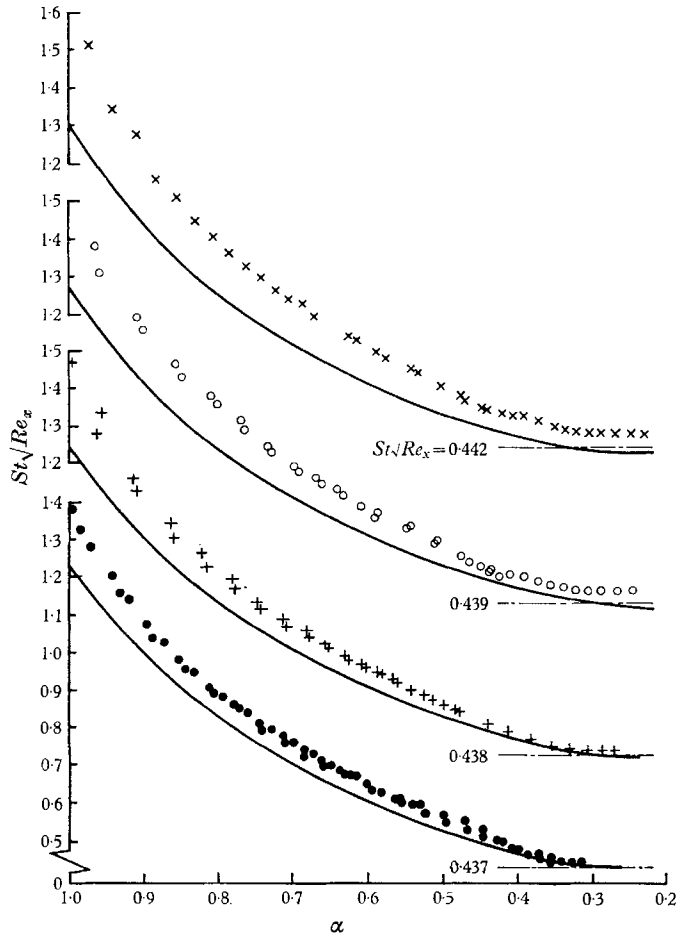

FIGURE 7. Comparison of experimental results at x = 34·9 mm with the analysis of Lam & Crocco. ×, W_{11} = 5·18, p_1/torr ∓ 5·5; ○, W_{11} = 4·8, p_1/torr = 8·5; +, W_{11} = 4·5, p_1/torr = 11·5; ●, W_{11} = 4·2. p_1/torr = 16·0; ——, $\rho\mu$ constant, Lam & Crocco (1958); — · —, $\rho\mu$ variable, steady flow asymptote, equation (15).

At low values of the Reynolds number, the heat transfer rate continues to diminish with time at any point on the plate. Even after the arrival of the leading edge particle (α = 1) at any station, the flow although inherently unsteady shows little change from the Mirels' type flow. The temperature begins to rise but slowly, while the heat transfer rate continues to fall (figure 6(*a*)) at a rate nearly proportional to (time)$^{-\frac{1}{2}}$.

This accords with the predictions of Lam & Crocco for the laminar boundary layer. The results in this region ($0 \leqslant \alpha \leqslant 1$) are shown in more detail in figure 7 where $St\sqrt{Re_x}$ is plotted aginst α for several values of shock Mach number and initial channel pressure. All the data in figure 7 are taken from transducers at

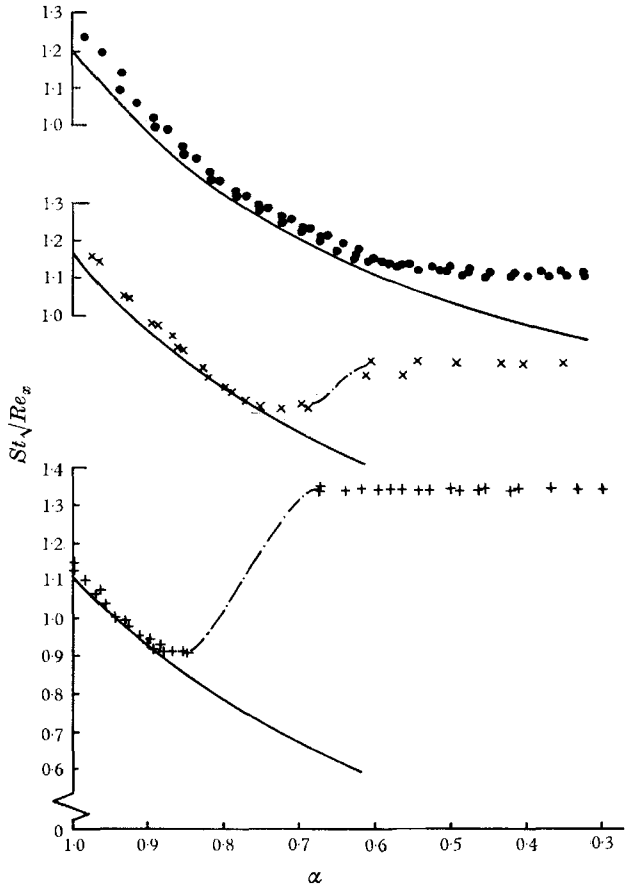

FIGURE 8. Comparison of experimental results at $x = 34{\cdot}9$ mm with the analysis of Lam & Crocco. ——, $\rho\mu$ constant, Lam & Crocco (1958); ●, $W_{11} = 3{\cdot}92$, p_1/torr $= 22$; ×, $W_{11} = 3{\cdot}52$, p_1/torr $= 34$; +, $W_{11} = 3{\cdot}06$, p_1/torr $= 61$.

positions on the plate over which the boundary layer is assumed to have remained laminar. It can be seen that $St\sqrt{Re_x}$ is substantially constant for $\alpha \gtrsim 0{\cdot}3$ as predicted. The absolute magnitudes of $St\sqrt{Re_x}$ differ by up to 20 % from the values computed by Lam. This discrepancy corresponds with that obtained in the quasi-steady, Mirels' type boundary layer, and is in part at least, accounted for by the assumption $\rho\mu =$ constant.

At higher Reynolds numbers the heat transfer rates depart more or less radically from the predictions of Lam & Crocco. It is inferred that the boundary layer was no longer laminar. Figures 8 and 9 show results in the range $\alpha \leqslant 1$ when the flow did not remain laminar. Figure 8 illustrates the effect of changing

shock Mach number and channel pressure for a fixed position on the plate. Figure 9 shows the conditions at several stations on the plate for constant flow conditions. Although $St\sqrt{Re_x}$ is not an appropriate parameter for a non-laminar boundary layer, it is, nevertheless, useful in showing departures from laminar flow; moreover constancy of $St\sqrt{Re_x}$ at any position on the plate (and hence constant Re_x) implies constant heat transfer rate. It is clear from figures 8 and 9 that when the boundary layer becomes non-laminar steady conditions are

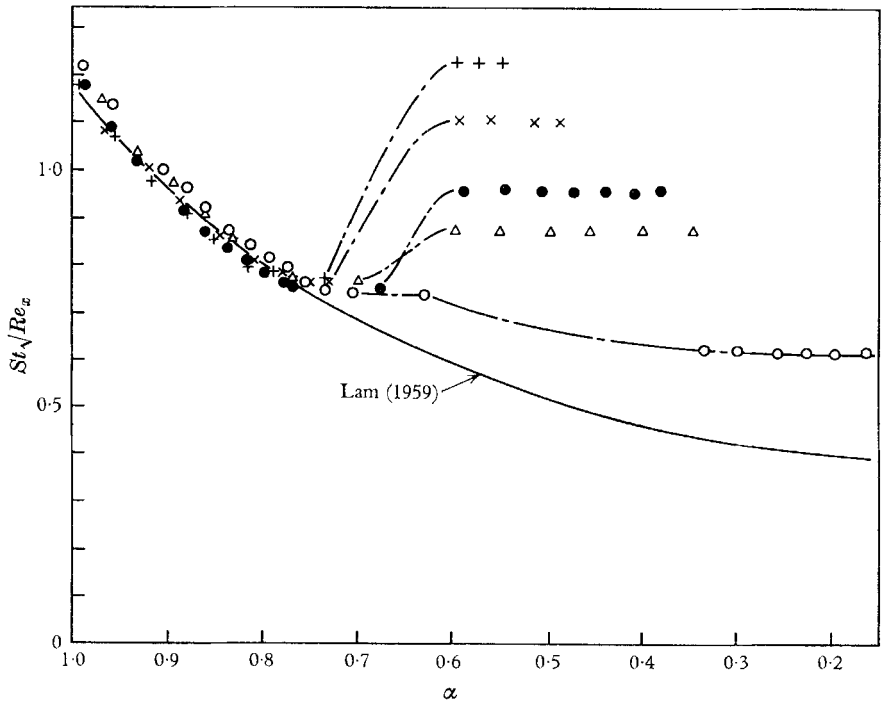

FIGURE 9. Superposition of results from several positions on the plate under nominally constant flow conditions. p_1/torr = 34: ○, W_{11} = 3·65, x/mm = 26·5; △, W_{11} = 3·51, x/mm = 34·9; ●, W_{11} = 3·56, x/mm = 44·0; ×, W_{11} = 3·50, x/mm = 53·1; +, W_{11} = 3·55, x/mm = 62·2.

reached earlier, that is at a greater value of α, than they would be in a laminar boundary layer. This agrees with the expectation that turbulent diffusion would provide a more rapid steadying influence than molecular diffusion. In order to gain further insight into the state of the boundary layer when it finally became steady, the final steady Stanton number was plotted against Re_x. This is shown in figure 10. The data conform to the 'familiar shape' indicating laminar, transitional and turbulent boundary-layer regions. In addition the steady Stanton number was also plotted against the Reynolds number Re_{x_s} based on the distance x_s behind the shock when this steady condition was *first attained* at any position on the plate (figure 11). The data are again seen to have the same familiar shape.

We shall return to these correlations in a later discussion. In the meantime we are now in a position to pick out several interesting features in the heat transfer

records, as depicted in figure 7 to 11. These are best illustrated on an (x, t) diagram and the systematic results of figure 9 for $W_{11} = 3{\cdot}5$ are replotted in this way on figure 12(a).

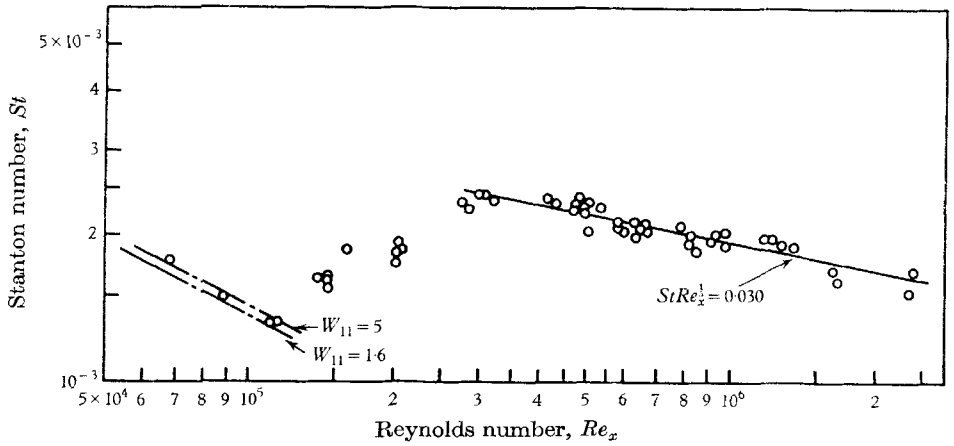

FIGURE 10. Correlation of the steady heat transfer rate with a Reynolds number based on the distance x from the leading edge of the plate. — - — - —, equation (15).

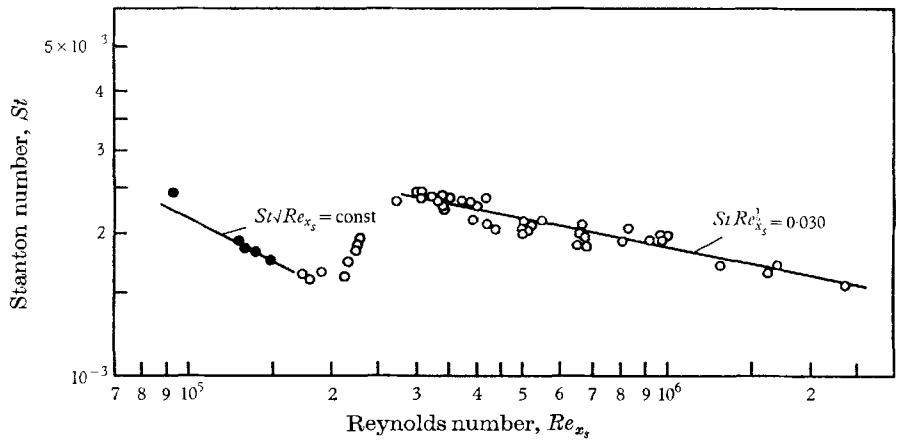

FIGURE 11. Correlation of the steady heat transfer rate with a Reynolds number based on the distance x_s between the shock and the transducer, when the boundary layer flow above the transducer first becomes steady. Also shown (●) are points for the quasi-steady laminar boundary layer.

In order to appreciate fully the significance of this diagram each of the lines drawn thereon will be discussed separately. (a) The first disturbance detected by any transducer is of course the arrival of the shock. This is the line $\alpha = w_1/u_2 = 1{\cdot}24$. ($b$) The line $\alpha = 1$ corresponding to the leading-edge particle path is shown. This divides the diagram into two domains. One of these, the Mirels' quasi-steady region $1 \leqslant \alpha \leqslant w_1/u_2$ is completely unaffected by anything which takes place in the second region $0 \leqslant \alpha \leqslant 1$. Almost the

entire quasi-steady region was laminar in this case. (*c*) The line $\alpha = 0{\cdot}57$ corresponds to the maximum *laminar* boundary-layer thickness at this shock Mach number, according to the results of Lam. (*d*) The line $\alpha = 0{\cdot}3$ is the approximate bound for the onset of steady laminar boundary-layer flow.

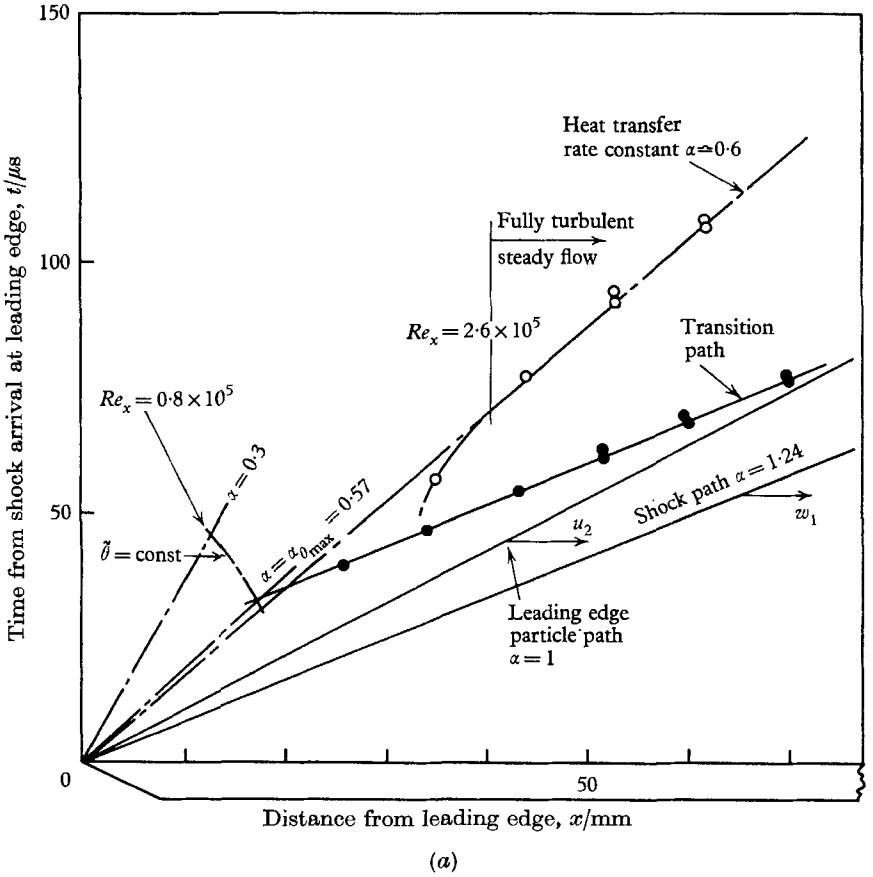

(*a*)

FIGURE 12. Correlation of results in the distance–time plane with particular reference to the behaviour of transition to turbulence. (*a*) $W_{11} = 3{\cdot}5$, $p_1 = 34$ torr. (*b*) $W_{11} = 2{\cdot}0$, $p_1 = 280$ torr.

(*e*) The 'transition path' shows the time at which the heat transfer rate departed from the regular behaviour which was assumed to correspond to laminar flow. This point could be readily inferred by plotting $\dot{q}_w$ *vs.* $(t - t_1)^{-\frac{1}{2}}$, see figure 6 (*b*). The transition path is seen to be more or less parallel to the shock path even in the inherently unsteady interaction region $\alpha \leqslant 1$. This corresponds with the results of Lam which indicate that the rate of diminution of $\dot{q}_w$ with time is little different from that in the quasi-steady region. In this latter region, as noted earlier, the boundary-layer thickness is defined by distance x_s from the shock, so that transition would be expected to follow a fixed distance behind the shock in any one set of test conditions. This has been confirmed by the work of Hartunian *et al.* (1960). (*f*) The intersection between the line $\alpha = 0{\cdot}57$ and the tran-

sition path is taken to correspond to the first point on the plate which experiences non-laminar flow in these conditions. At this point, the boundary-layer momentum thickness $\tilde{\theta}$ first reaches its critical value $\tilde{\theta}_{\text{crit}}$. A line $\tilde{\theta} = \tilde{\theta}_{\text{crit}}$ is drawn, using Lam's results, between $\alpha = 0{\cdot}57$ and $\alpha = 0{\cdot}3$. Transition is expected

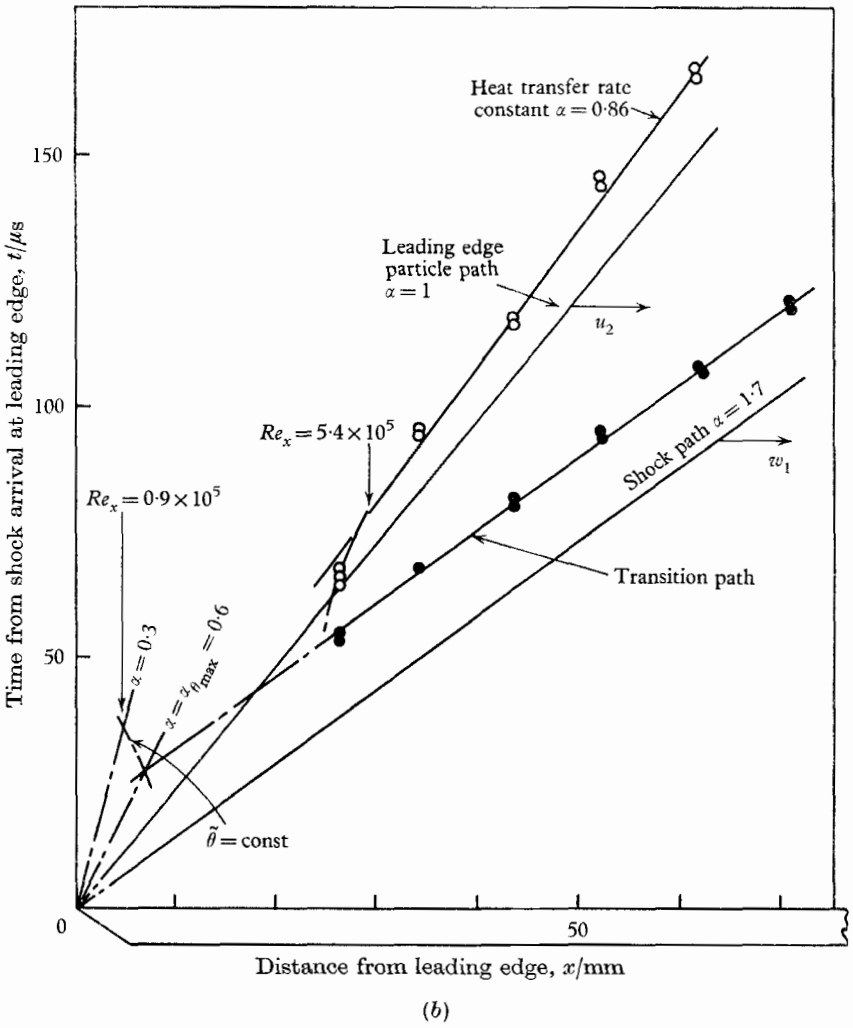

(*b*)

FIGURE 12*b*. For legend see previous page.

to move upstream along some such path as discussed in § 2. The Reynolds number Re_x corresponding to this forwardmost appearance of non-laminar flow is indicated. (*g*) Finally, a line is drawn joining those points (open circles) which denote the attainment of *steady, non-laminar* flow. Part of this line is a straight line $\alpha = \alpha_F$ which passes through the origin of the (x, t) plane. It is found that all those points which lie on $\alpha = \alpha_F$ have values of St and Re_x such that they correspond to a fully developed turbulent boundary layer as inferred from the correlation of figure 10. Moreover those points not on $\alpha = \alpha_F$ have values which accord-

ing to figure 10 are appropriate to the steady transitional boundary layer. The downstream limit of this steady transitional boundary layer has been estimated on the diagram and the corresponding value of Re_x is indicated. We are thus able to infer the steady 'transition-length' x_{tr} under these conditions (wall to free-stream temperature ratio $T_w/T_2 = 0{\cdot}31, M_2 = 1{\cdot}54$) as corresponding to a Reynolds number range $0{\cdot}8 \lesssim Re_{xtr} \times 10^{-5} \leqslant 2{\cdot}6$.

Figure 12(*b*) shows an (x,t) diagram for a shock Mach number $W_{11} = 2$.† The trends are similar but here the transition path lies in the quasi-steady domain. The transition length Reynolds number range for this case

$$(T_w/T_2 = 0{\cdot}593, M_2 = 0{\cdot}97) \quad \text{is} \quad 0{\cdot}9 \lesssim Re_{xtr} \times 10^{-5} \lesssim 5{\cdot}5.$$

This method of determining the length of the transitional boundary layer warrants further investigation, since it seems to define it within fairly narrow limits.

One feature of figures 12(*a*) and (*b*) is that $\alpha_F \approx \frac{1}{2}w_1/u_2$. That this is a 'general (empirical) result' may be demonstrated in the following way. The turbulent boundary-layer data are correlated in figures 10 and 11 by approximate relations of the form

$$St(Re_x)^{n_1} = C_1 \quad \text{when} \quad \dot{q}_w = \text{constant}$$

and

$$St\,(Re_{x_s})^{n_2} = C_2 \quad \text{when } \dot{q}_w \text{ first reaches its steady value.}$$

Both these relations are applicable to that point at which the turbulent boundary layer is first steady and hence we may determine the corresponding values of x ($= x_F$, say) and x_s ($= x_{sF}$). Within the experimental error, $n_1 = n_2 = 0{\cdot}2$ and $C_1 = C_2 = 0{\cdot}030$ so that

$$x_s = x_{sF};$$

that is, when part of the steady boundary layer is fully turbulent *half of the total boundary-layer length is steady* (with the possible exception of a small region in the transitional boundary layer). It follows that

$$\alpha_F = \tfrac{1}{2}w_1/u_2.$$

The implication is that stronger shocks (lower w_1/u_2) require longer times to produce steady turbulent boundary layers. In the context of the shock tube as a wind tunnel device, this is a disadvantage, since the available test time decreases severely with increasing shock strength.

It remains to compare the steady turbulent heat transfer rate data with previous data correlations. To a large extent one is handicapped here because the vast majority of workers have been concerned with skin friction measurements (see, for example, Spalding & Chi 1964) and in order to predict heat transfer rates a Reynolds analogy factor Ra is required.

According to Spence (1960) a Reynolds analogy factor of 1·18 is an appropriate value for the present conditions. When this value is used in conjunction with his

† For the chamber/channel length ratio of this shock tube, the head of the reflected rarefaction is expected to overtake the shock near the model at this shock strength when a hydrogen/nitrogen combination is used. No evidence of this was detected in the heat transfer rate records, but the corresponding pressure and temperature changes would be very small over the time scale of interest here.

correlation for skin friction data, based upon the mean enthalpy concept, (17) is obtained. The experimental data of figure 10 have been recomputed taking account of the laminar and transitional boundary layer ahead of the turbulent region by estimating a 'false origin' for the latter. In addition the heat transfer rate coefficient and the Reynolds number have been calculated using the gas properties evaluated at the mean enthalpy given by (18). The data together with Spence's 'prediction' are plotted in figure 13.

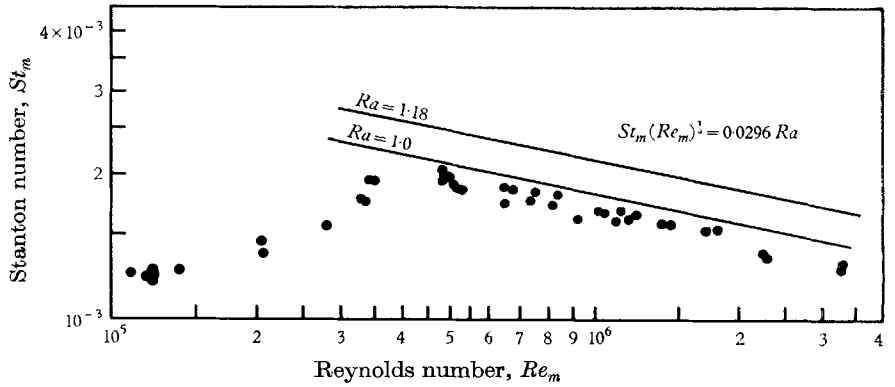

FIGURE 13. Correlation of data using the mean enthalpy method. The distance x_T used in the Reynolds number Re_m has been corrected to take account of the false origin of the turbulent boundary layer.

The data show somewhat less scatter than is apparent in figure 10, but they fall some 20 % below Spence's curve. If his correlation of the skin-friction data is regarded as acceptable, a Reynolds analogy factor closer to unity would seem more realistic, see figure 13. This would correspond to a 'turbulent Prandtl number', σ_{turb}, equal to unity which has been argued as a reasonable value on the grounds that energy and momentum transfer both take place largely as a result of turbulent mixing.

Some further support for this value is given by the results of Wallace (1967) who measured skin friction and heat transfer rates simultaneously in a hypersonic shock tunnel flow. His data were taken at somewhat higher Reynolds numbers and flow Mach numbers than those reported here and, although his values of wall to freestream temperature ratios are different, the ratios of T_w to stream stagnation temperature are similar. Although Wallace's results show some scatter, his values of Ra are on average, only slightly above unity. There remains more than sufficient uncertainty, however, to warrant a systematic investigation of this matter.

4. Concluding remarks

The experimental results reported in §3 have clearly established the overall reliability of the laminar theory due to Lam & Crocco. Further evidence has been presented supporting the quasi-steady laminar boundary-layer theory of Mirels for the boundary layer in the neighbourhood of the shock.

The transition to turbulence in this inherently unsteady boundary layer has also been examined experimentally. Phenomenological arguments are put to explain this transition process and the measured data are shown to provide circumstantial evidence in support of these arguments. Steady heat transfer rates have also been measured in the laminar, transitional and turbulent boundary layers.

The approach to steady conditions has been discussed in relation to its bearing on the available test time in the uniform hot flow behind the shock in a shock tube. For the laminar boundary layer with zero pressure gradient the flow is substantially steady at a distance x from the leading edge of the plate after a time t given by

$$t = x/0{\cdot}3u_2,$$

where t is measured from the instant of shock arrival at $x = 0$. This accords with theory.

When the boundary layer is turbulent, it has been discovered empirically that half the boundary-layer length is steady. That is, the flow over a flat plate should have a steady boundary layer when the shock initiating the motion is about one chord downstream of the trailing edge. This implies that the length of the test gas sample in a shock tube, that is the distance between the shock and contact region, should be at least two model chord lengths. When pressure gradients exist or flow separation occurs this may be insufficient. The requirements under these circumstances need investigating.

The steady laminar heat transfer rates show fairly good agreement with the predictions of Crocco as approximated by Young (1953). The turbulent data correlate with Spence's relation based on a mean enthalpy concept only if a Reynolds analogy factor close to unity is used. Spence himself suggests a rather higher value than this, but there is evidence (Wallace 1967) that a value of unity is not unrealistic. If this is so, Spence's skin-friction values would apply, though Wallace found rather lower values in his experiments than those given by Spence's relation. This aspect of the work needs further investigation.

The authors would like to express their gratitude to the Ministry of Technology who supported this work under an extra-mural agreement.

REFERENCES

Ackroyd, J. A. D. 1967 On the laminar compressible boundary layer induced by the passage of a plane shock wave over a flat wall. *Proc. Camb. Phil. Soc.* **63**, 889.

Bernstein, L. 1963*a* Notes on some experimental and theoretical results for the boundary layer development aft of the shock in a shock tube. *Aero. Res. Coun.* C.P. no. 625.

Bernstein, L. 1963*b* Tabulated solutions of the equilibrium gas properties behind the incident and reflected normal shock wave in a shock tube. *Aero. Res. Coun.* C.P. no. 626.

Bernstein, L. & Goodchild, R. O. 1967 High sensitivity piezoelectric transducer for wave velocity measurements in shock tubes. *Rev. Sci. Instrum.* **38**, 971.

Carslaw, H. S. & Jaeger, J. C. 1947 *Conduction of Heat in Solids.* Oxford: Clarendon Press.

Davies, W. R. 1968 Ph.D. Thesis. London University.

DEM'YANOV, U. A. 1957 Boundary layer formation on a plane with a moving shock wave. *J. Priklad. Math. Mech.* **21**, no. 3.

HARTUNIAN, R. A., RUSSO, A. L. & MARRONE, P. V. 1960 Boundary layer transition and heat transfer in shock tubes. *J. Aerospace Sci.* **27**, 587.

HOWARTH, L. 1951 Some aspects of Rayleigh's problem for a compressible fluid. *Quart. J. Mech. Appl. Math.* **4**, 157.

LAM, H. 1959 Numerical solutions of shock induced unsteady boundary layers. *Princeton University Report*, no. 480.

LAM, H. & CROCCO, L. 1958 Shock induced unsteady laminar compressible boundary layers on a semi-infinite flat plate. *Princeton University Report*, no. 428. Also *J. Aerospace Sci.* **26** (1959), 54.

MEYER, R. F. 1960 A heat flux meter for use with thin film surface thermometers. *N.R.C. Ottawa Report* L.R. 279.

MIRELS, H. 1955 Laminar boundary layer behind a shock wave advancing into a stationary fluid. *N.A.C.A.* TN 3401.

MIRELS, H. 1956 Boundary layer behind a shock or thin expansion wave moving into a stationary fluid. *N.A.C.A.* TN 3712.

MIRELS, H. 1961 Laminar boundary layer behind a strong shock moving into air. *N.A.S.A* TN-D 291.

RAYLEIGH, LORD 1911 On the motion of solid bodies through viscous fluids. *Phil. Mag.* **6**, 21.

SPALDING, D. B. & CHI, S. W. 1964 The drag of a compressible turbulent boundary layer on a smooth flat plate with and without heat transfer. *J. Fluid Mech.* **18**, 117.

SPENCE, D. A. 1960 Velocity and enthalpy distributions in the compressible turbulent boundary layer on a flat plate. *J. Fluid Mech.* **8**, 368.

SPENCE, D. A. & WOODS, B. A. 1960 Boundary layer and combustion effects in shock tube flows. Paper in *Hypersonic Flow*. Ed. J. Tinkler. London: Butterworths.

STEWARTSON, K. 1951 On the impulsive motion of a flat plate in a viscous fluid. *Quart. J. Mech. Appl. Maths.* **4**, 182.

STEWARTSON, K. 1955 On the motion of a flat plate at high speed in a viscous compressible fluid. Part I. Impulsive motion. *Proc. Camb. Phil. Soc.* **51**, 202.

WALLACE, J. E. 1967 Hypersonic turbulent boundary layer studies at cold wall conditions. *Proc. of Ht. Transfer and Fluid Mech. Inst.* Stanford, California: Stanford Univ. Press.

WOOLLEY, H. W. 1956 Thermodynamic properties of gaseous nitrogen. *N.A.C.A.* TN 3217.

YOUNG, A. D. 1953 *Modern Developments in Fluid Dynamics—High Speed Flow*, vol. 1. Oxford University Press.

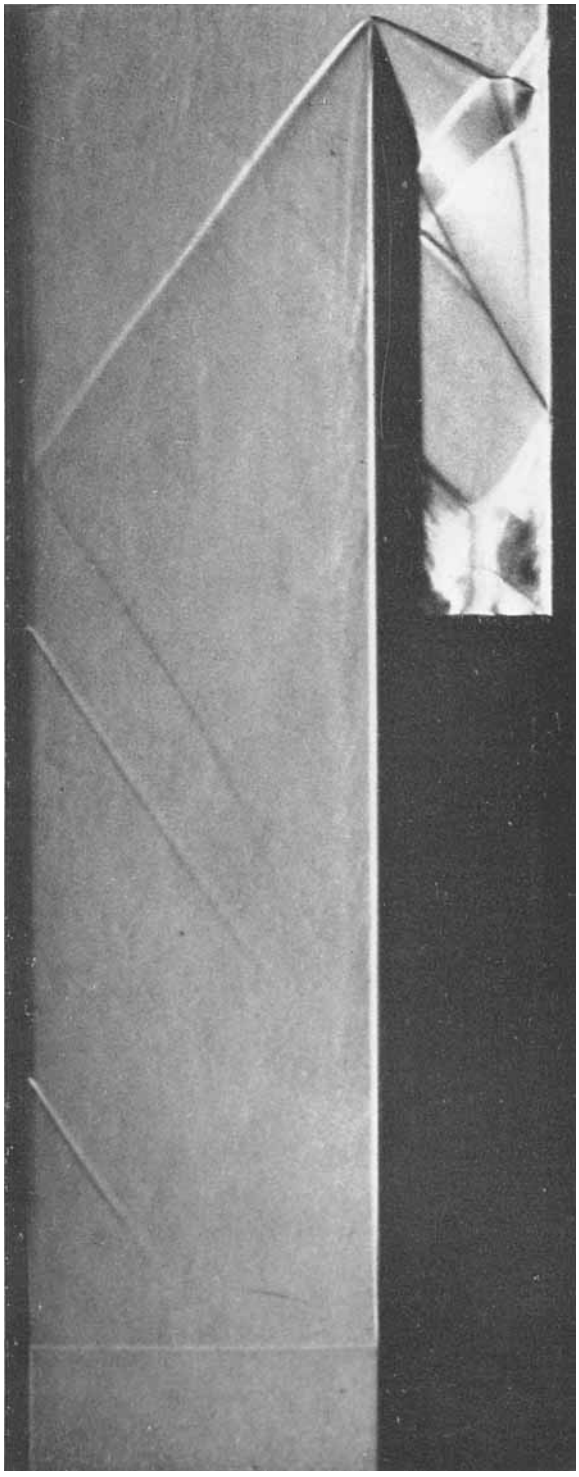

FIGURE 14. Schlieren photograph of the shock induced flow over a semi-infinite flat plate at a shock Mach number of 5·3. The undisturbed channel pressure is 10 torr N_2. (The waves emanating from the upper wall arise from an imperfectly fitting model-mounting blank.)

(*Facing p.* 112)